

External Flow Past a Cylinder

1. INTRODUCTION

The aim of this study is to study the external flow past a cylinder. This is a field of interest as it represents bluff body flow which has many applications in field of engineering. The fixed cylinder problem is notable research topic in Computational Fluid Dynamics (CFD) [1]. Despite the simplicity of geometry and input parameters, the nature of the flow complicates the calculation. The behaviour of flow over a cylinder changes drastically as the intensity of flow varies. Karman Vortex sheet effect on a cylinder can be seen as low at $Re=47$ [2]. As turbulence increases, the beginning of transition shifts upstream, about the separation point. Alongside, large eddies start to form nearby to the cylinder's base. [1].

In this study, we were tasked to create a 2D axisymmetric geometry of a cylinder in a fluid domain. The cylinder has a fluid flowing past it at a free stream velocity at U_{∞} . Pressure coefficient (C_p) around one half of perimeter of the cylinder from point A (Stagnation point – 0°) to point B (180°) was to be stimulated using Ansys. A 2D axisymmetric model is used because of symmetry of the cylinder and to reduce complexity and computational time. The free stream velocity is calculated based on the Reynolds number of 3900.

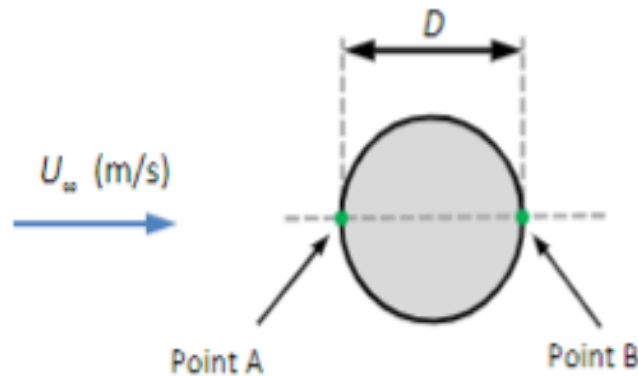


Figure 1 Cylinder geometry

The results are to be compared with the experimental data generated by Kravchenko et al [3] and by utilising the theoretical inviscid solution which is given by equation (1).

$$C_p = 1 - 4\sin^2\theta$$

1

Kravchenko et al [3] studied the flow over cylinder at $Re = 3900$ using large eddy simulation (LES) technique. In their study, the computations were conducted with a high-order precise numerical method based on *B*-splines and compared with previous upwind-biased and central finite-difference simulations and with the existing experimental data [3]. In the near wake region all 3 simulations are in conjunction with each other, but it's further downstream where the *B*-spline computations are in better agreement with the experimental results.

In this study, simulations were ran utilising an 2D axisymmetric model and its results are compared with experimental and numerical data.

2. GEOMETRY

As mentioned earlier, a 2D axisymmetric geometry is to be created such that only one half of the fluid is to be modelled. The Domain and Diameter of the cylinder dimensions can be chosen individually. In CFD, the domain plays a vital role in achieving of valid results and any changes to the domain could lead to changes in results. Here, the dimension of domain depends on the diameter of the cylinder and the domain should be big enough for the development of flow before being incident on the cylinder and should be big enough for the capturing of flow separation and eddies to be performed after flow separation downstream.

The Diameter of the domain is 1m in length which would make the height of the fluid $10D = 10m$ (As provided in assignment) and the length in streamwise direction is $15D = 15m$ (Excluding the cylinder). The length before cylinder is set to be $5m$ for fully developing the flow and in the wake region downstream the length is set to be $10m$ for capturing the development of the eddies.

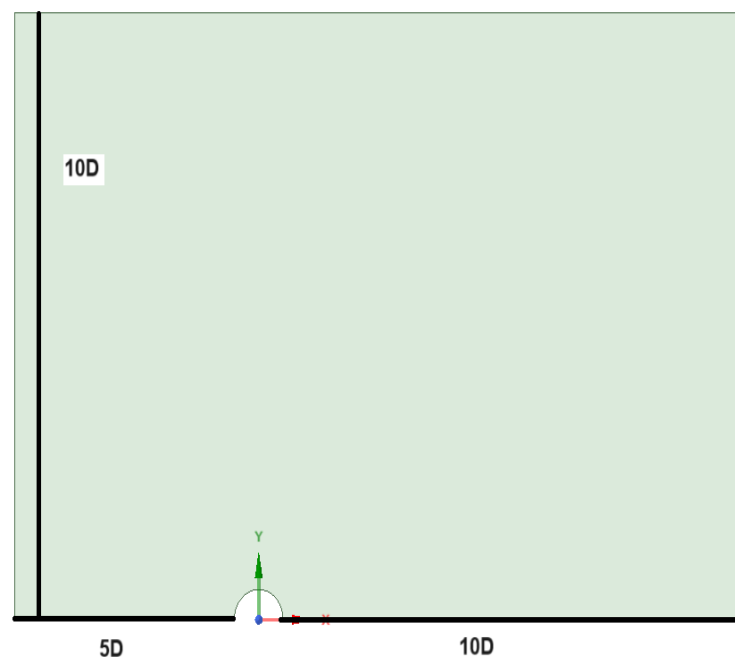


Figure 2 Sketch of the computational domain

3. BOUNDARY CONDITIONS

For obtaining optimum results and the flow analysis the boundary conditions should be defined effectively. Defining the boundary conditions for the external flow past a cylinder is a pivotal step in capturing the bluff-body flow physics precisely. The boundary conditions chosen should copy the physical behaviour of the fluid in the real-world conditions, ensuring that the simulation provides deep understandings.

According to the physics features the left side is marked as inlet and right side is marked as outlet. The walls are marked at the top and surface of cylinder is considered as no-slip wall.

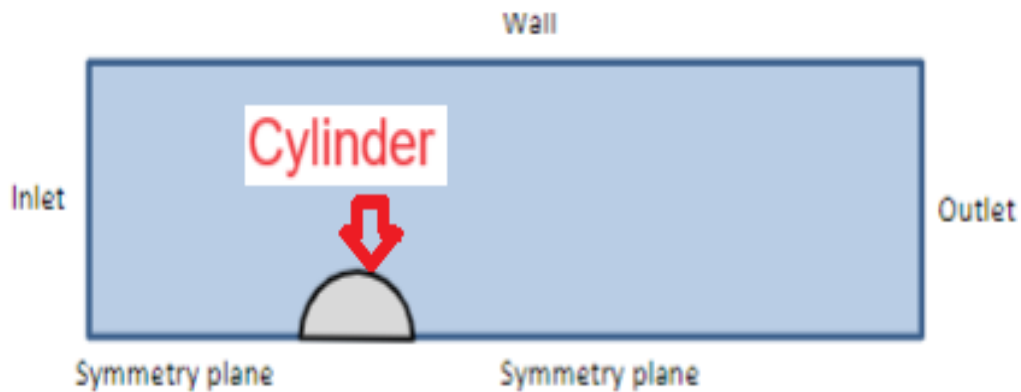


Figure 3 Boundary Conditions

3.1 Inlet Boundary Conditions

Normally, a velocity-inlet condition is used to define the flow at the inlet. The inlet velocity is calculated such that the simulated airflow is with a Reynolds number of 3900.

$$Re = \frac{\rho U_{\infty} H}{\mu} \quad (2)$$

Eq. 2 is used to calculate the Free stream velocity. Here, the known terms are

Re (Reynolds No.) = 3900

ρ (Density) = 1.225 Kg/m³

μ (Dynamic Viscosity) = 1.7894e⁻⁴ Kg/ms

H (Characteristic length) = 0.5m

Using the above mentioned the calculated free stream velocity is 0.1175 m/s to stimulate 3900 Reynolds No. flow. Using the Reynolds no. turbulent intensity is calculated to be 0.057%.

$$l = 0.16(Re_{DH})^{-\frac{1}{8}} \quad (3)$$

The turbulent length scale is taken as the diameter of the cylinder, i.e. = 1m.

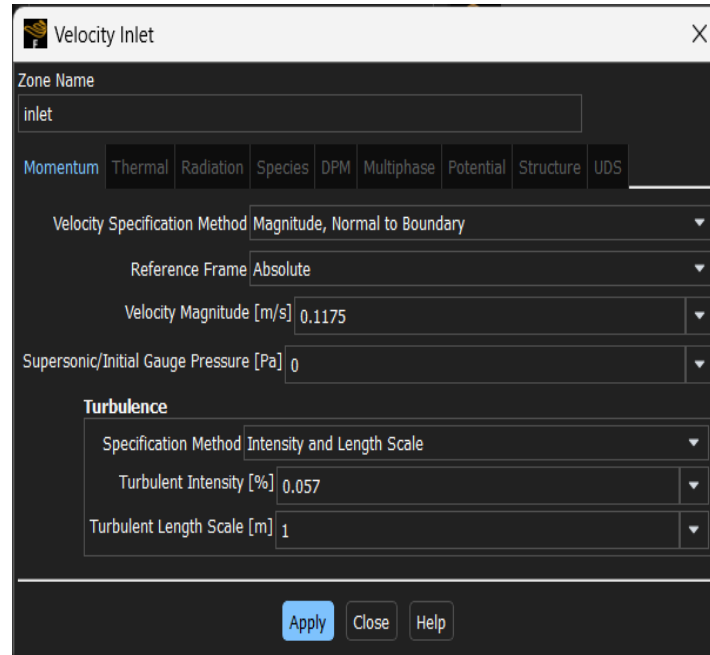


Figure 4 Inlet Boundary Conditions

3.2 Wall Boundary Conditions

Wall boundary conditions determine the interaction between the fluid and the solid surfaces within the domain. As the flow is developing to be turbulent the wall near wall condition for study of flow is of paramount importance. To study the near wall function accurately the mesh needs to be developed such it is focused primarily on the cylinder wall and is below the required y^+ value of the model used. As the model used is SST K-omega which needs maximum of 1 y^+ value, the maximum y^+ for all the meshes generated is showcased in the table 1:

Table 1

Type	y^+ value
Finest	0.1855874
Finer	0.2160427
Medium	0.2592344
Coarser	0.2983791
Coarsest	0.3175412

3.3 Outlet Boundary Conditions

Normally, for the outlet, pressure-outlet condition is used. These conditions sustain the static pressure at the outlet, allowing for regular pressure gradients within the area. Here, the gauge pressure is set to be zero to replicate the outer real-world pressure. As we have assumed that the inlet and outlet are squares the Reynolds no. wouldn't change during the simulation, Turbulence intensity is calculated the same way we did for inlet. The backflow turbulent length scale is taken as the diameter of the cylinder, i.e. = 1m.

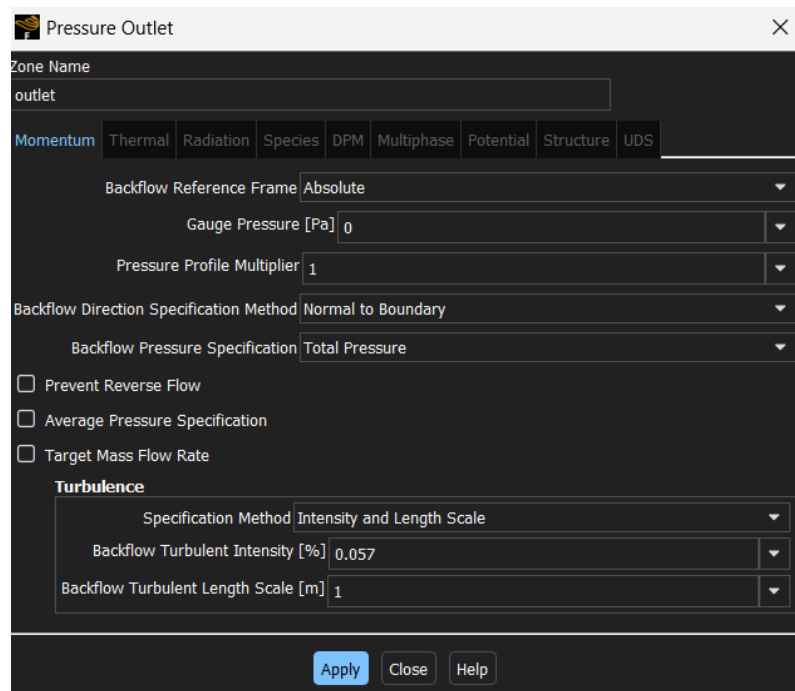


Figure 5 Outlet Boundary Conditions

3.4 Turbulence model

We know LES and Direct Numerical Simulation (DNS) techniques are more accurate than RANS (Reynolds-Averaged Navier-Stokes), but they are also very complex and computationally demanding techniques. Which results in extremely complex and detailed designs and longer simulations time. As the Reynolds no. of 3900 is close to turbulence and flow is transitioning towards turbulent from being laminar LES will be the model which would be ideal as it will be lower in computational cost than DNS and higher in accuracy than RANS. But, for present scenario K-omega SST model is utilised to run the simulations and get a close to accurate result. This model may not match the accuracy of LES or DNS for obtaining complete unsteady flow phenomena, but it provides a realistic approximation with much lower computational requirements. The k-omega model focuses on solving time-averaged equations. It predicts the turbulent flow by solving 2 transport equations:

1. One for turbulence kinetic energy

2. One for specific dissipation rate.

So, to achieve a close enough approximation, k-omega SST model is utilised to achieve the results.

4. MESH DESIGN

The mesh, also referred to as the grid, is the discretization of the computational domain into a collection of small elements or cells. Defining Mesh plays an important role in accuracy and reliability of the simulations in CFD. A more detailed description regarding meshing is mentioned below:

An unstructured mesh is chosen in the present study. As shown in figure – 6, mesh design around the cylinder is generated by utilizing triangular grids. The max first layer thickness of 2.0931mm was kept around the cylinder to attain the maximum y^+ value of 0.3175412, in the 5 meshes generated to attain mesh independence. The finest mesh didn't get the best agreement with experimental values. Finally, a mesh of 42,072 elements was generated which attained the best agreement with the experiment values and had the average skewness and y^+ value of 0.073673 and 0.2592344 respectively.

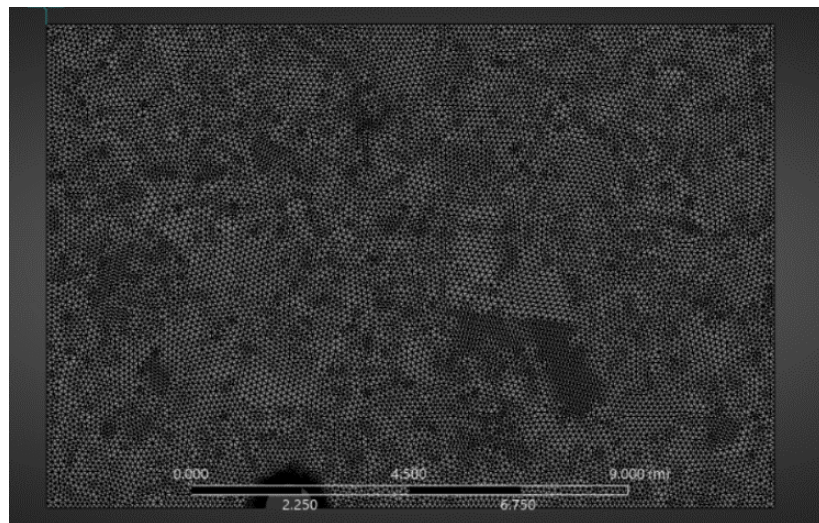


Figure 6 Global mesh

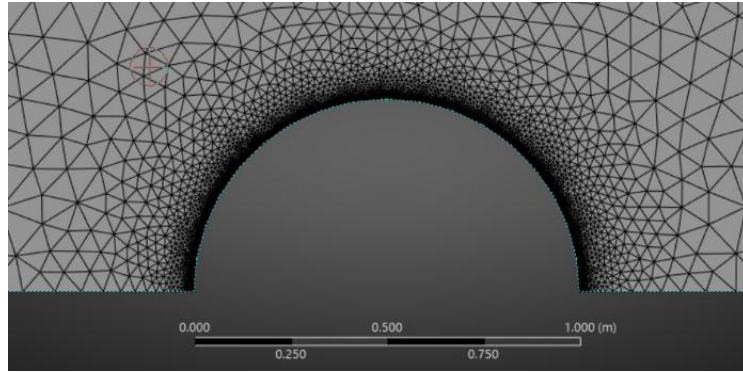


Figure 7 Local Mesh

4.1 MESH INDEPEDENCE STUDY

Mesh independence study is a vital in determining the reliability and accuracy of the CFD simulations. In such study, refinement of mesh is done such that the created meshes produce converged result towards a consistent solution, irrespective of the grid resolution. Here, the objective is to verify the optimal mesh that delivers accurate solutions without unnecessarily increasing computational cost.

In the present study, 5 different meshes were generated, varying in grid resolution. Their y^+ value, convergence steps, C_p error percentage, skewness and grid size were examined across the different mesh densities to evaluate mesh independence.

Table 2 Mesh Independence

Type	Total Elements	Y^+ value	Convergence Steps	C_p Error %	Average Skewness
Finest	77,469	0.1855874	103	38.925	0.06452
Finer	56,466	0.2160427	102	24.832	0.06961
Medium	42,072	0.2592344	96	20.304	0.07367
Coarser	31,313	0.2983791	97	33.169	0.07641
Coarsest	24,599	0.3175412	98	22.959	0.07760

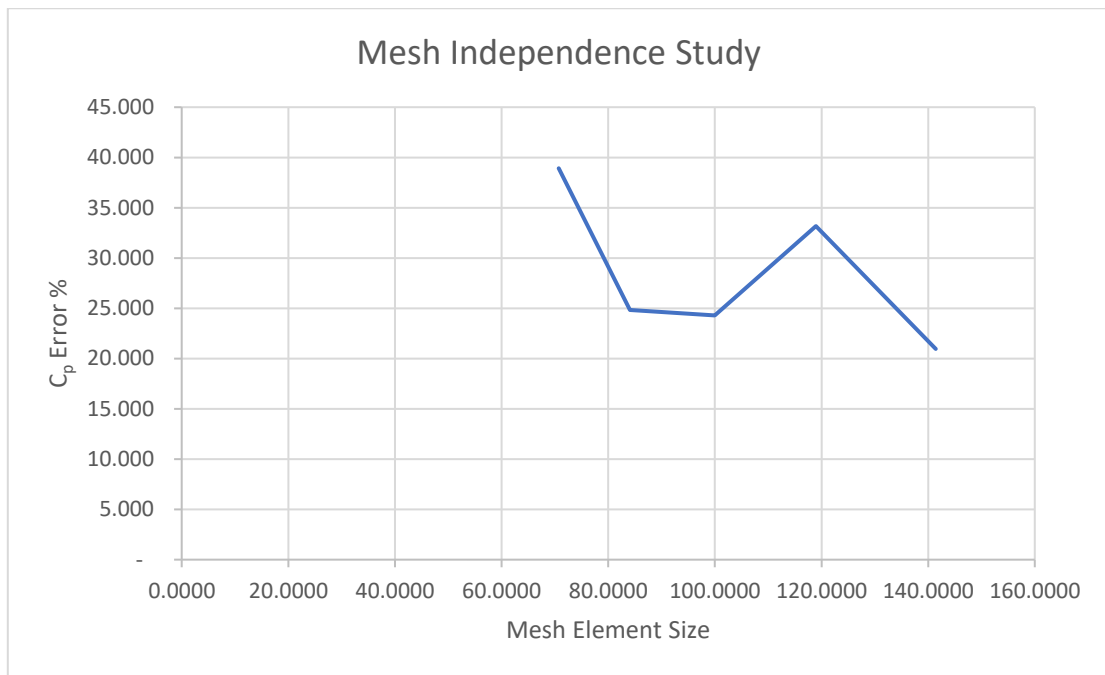


Figure 8 Mesh Independence Study

- **Finest Mesh:** It has the smallest mesh element size of 70.7107mm and highest no. of elements at 77,469, but it also has the highest C_p error percentage when compared to the experimental values.
- **Finer Mesh:** Compared to the finest mesh it has a slightly larger mesh element size of 84.0896mm and a total of 56,466 elements, this showcases a reduction in C_p error percentage to 24.832%. With a slight increase in y^+ value, the capturing of boundary layer effect has increased.
- **Medium Mesh:** It has a total mesh element size of 100mm and a total of 42,072 elements. With a C_p error percentage of 20.304%, it has the lowest error percentage of all the meshes and the y^+ value of 0.2592344 which is in the acceptable range for the k-omega SST model. The convergence steps of 96 was like that of the finer mesh, implying that further refinement may not extensively affect the results
- **Coarser Mesh:** It has the mesh size slightly increased to 118.9207mm and total elements of 31,313. With the C_p error percentage of 20.304% and y^+ value of 0.2983791.
- **Coarsest Mesh:** It has the largest mesh element size of 141.4214mm and total element size of 24,599. With the C_p error percentage of 22.959% and y^+ value of 0.3175412.

The average skewness value beyond all the mesh, were within the acceptable range. Indicating that, the different mesh generated are refined and do not affect the accuracy of the simulations.

This study showcases that although finer meshes provided enhanced near-wall resolution, they do not always yield the most accurate C_p results. The C_p error decreased with coarser meshes, up to a certain point, outside which further coarsening lead to inaccuracies. Here, the medium mesh strikes a balance among computational efficiency and accuracy, with an acceptable C_p error and skewness values.

5. RESULTS AND ANALYSIS

In this section, the analysis of results obtained from the simulations of external flow over a cylinder at Reynolds No. of 3900 are discussed. Here, the C_p data obtained from RANS model simulations, experimental data and numerical calculations is compared.

In figure – 9 the flow separation over the cylinder surface has been showed. The flow separation occurs almost 90° from the stagnation point, where the free stream velocity is zero and has maximum pressure. The separation angle is even with the anticipated behaviour of the flow in the transitional flow regime at this Reynolds number. The separation of flow occurs, due to high pressure gradient, which leads to wake being formed downstream of the cylinder. This is a vital phenomenon as it influences both pressure distribution and drag experienced by the cylinder.

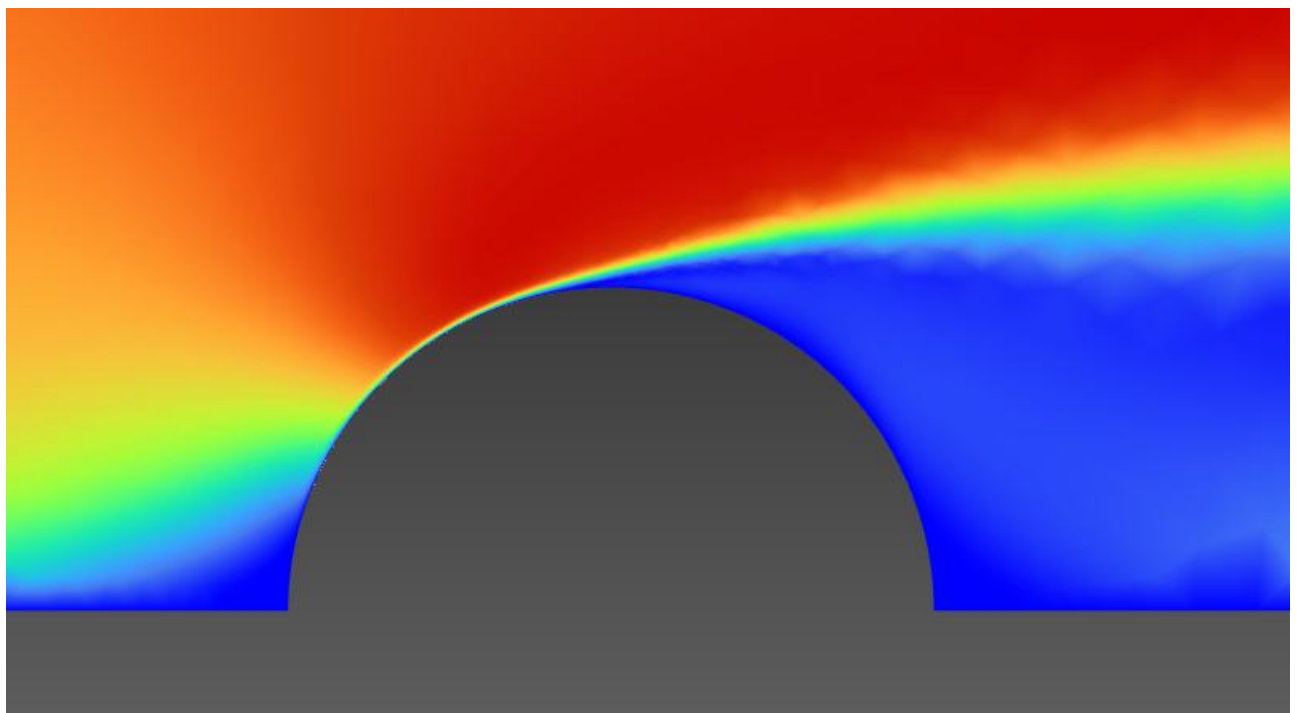


Figure 9 Flow separation

Figure – 10 showcases the pressure distribution across the domain. Around the stagnation point (Point A - 0°) and decreases along the surface as the flow accelerates around the cylinder, reaching a minimum in the wake region downstream the cylinder.

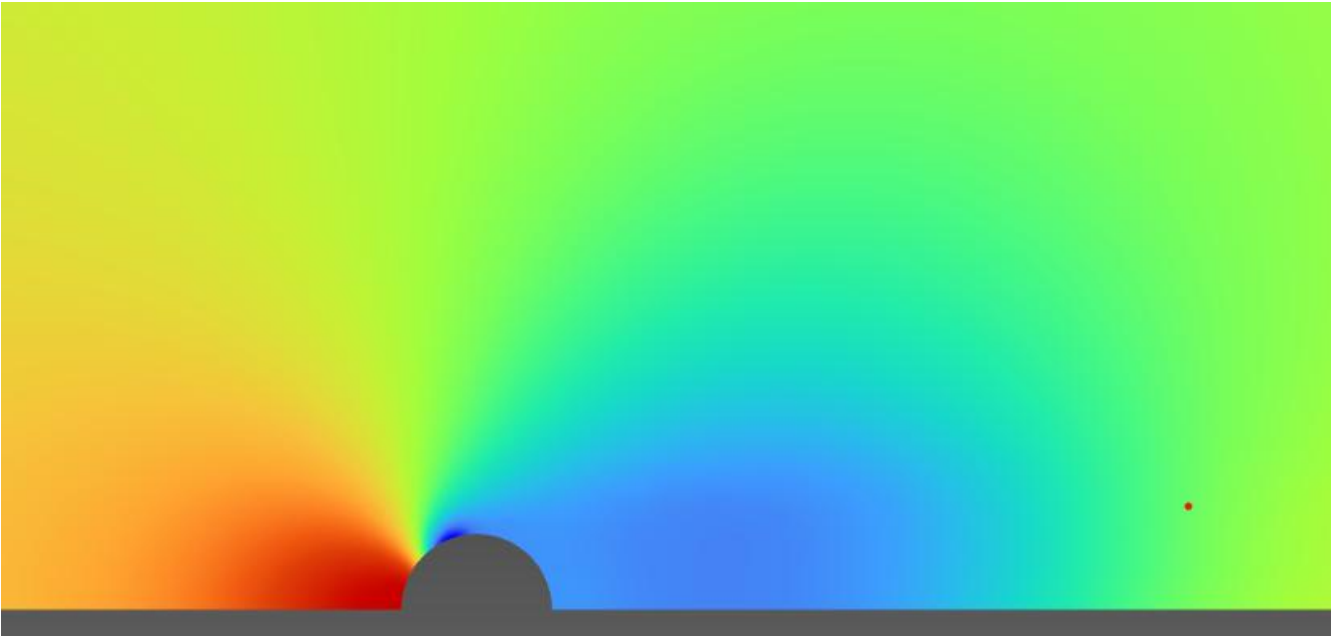


Figure 10 Pressure Variation

5.1 DATA COMPARISION

In this section we will compare the data obtained from simulations with the experimental and numerical values. The experimental data has been provided and theoretical values are generated using equation (1). The inviscid solution, represented by Equation (1), provides the ideal case for a cylinder in external flow, avoiding the effects of viscosity and flow separation. While, the experimental and simulation data, reason for the real-world effects of viscosity, boundary layer development, and flow separation.

- **THEORETICAL INVISCID SOLUTION** – The theoretical values are generated using equation (1). Here, θ – Angular position on the cylinder's surface from the stagnation point.

$$C_p = 1 - 4\sin^2\theta \quad 1$$

The assumption of this equation is that there are no viscous forces acted on the fluid. Thus, no boundary layer development or flow separation takes place. The distribution of pressure is symmetric about the stagnation point (Point A) and rear of cylinder (Point B).

- **EXPERIMENTAL DATA** – The experimental data is obtained from karavchenko et.al. [3] who conducted numerical studies of external flow over a cylinder at $Re = 3900$. In this study, LES model was used to generate the result.
- **NUMERICAL SIMULATIONS** – The numerical simulations data which were conducted by utilising RANS based K-omega SST model are represented in this section.

At the stagnation point (Point A) $C_p = 1$ for all three data sets as this point the velocity is zero and pressure is at maximum. At smaller angles of $\theta < 40^\circ$, both the theoretical and experimental data follow a similar trend of decrease in C_p due to presence of boundary layer. While the numerical data showcases a more aggressive decrease in C_p , indicating that the k-omega SST model predicts earlier flow disturbances and higher velocity gradients compared to both the other data sets.

At $\theta=80^\circ-100^\circ$, where from figure-9 flow separates visibly, theoretical solution suggests that C_p value decreases symmetrically, indicating no flow separation. While the experimental data shows a sudden decline in C_p indicating flow separation. This drop is steadier matched against the numerical data, which calculates an earlier and more acute separation, implying greater turbulence effects calculated by the model.

In the wake region i.e. $\theta>100^\circ$, the theoretical calculations, ignores the wake effects and shows a smooth pressure recovery. The experimental data indicates the lower C_p value in the wake region, which is consistent with the flow separation downstream of the cylinder. In comparison with both the data sets, numerical simulations show more steeper pressure drop, suggesting that CFD model might be overpredicting the strength and extent of pressure drop in the wake compared to experimental data.

The above discussion is about the below presented figure – 11.

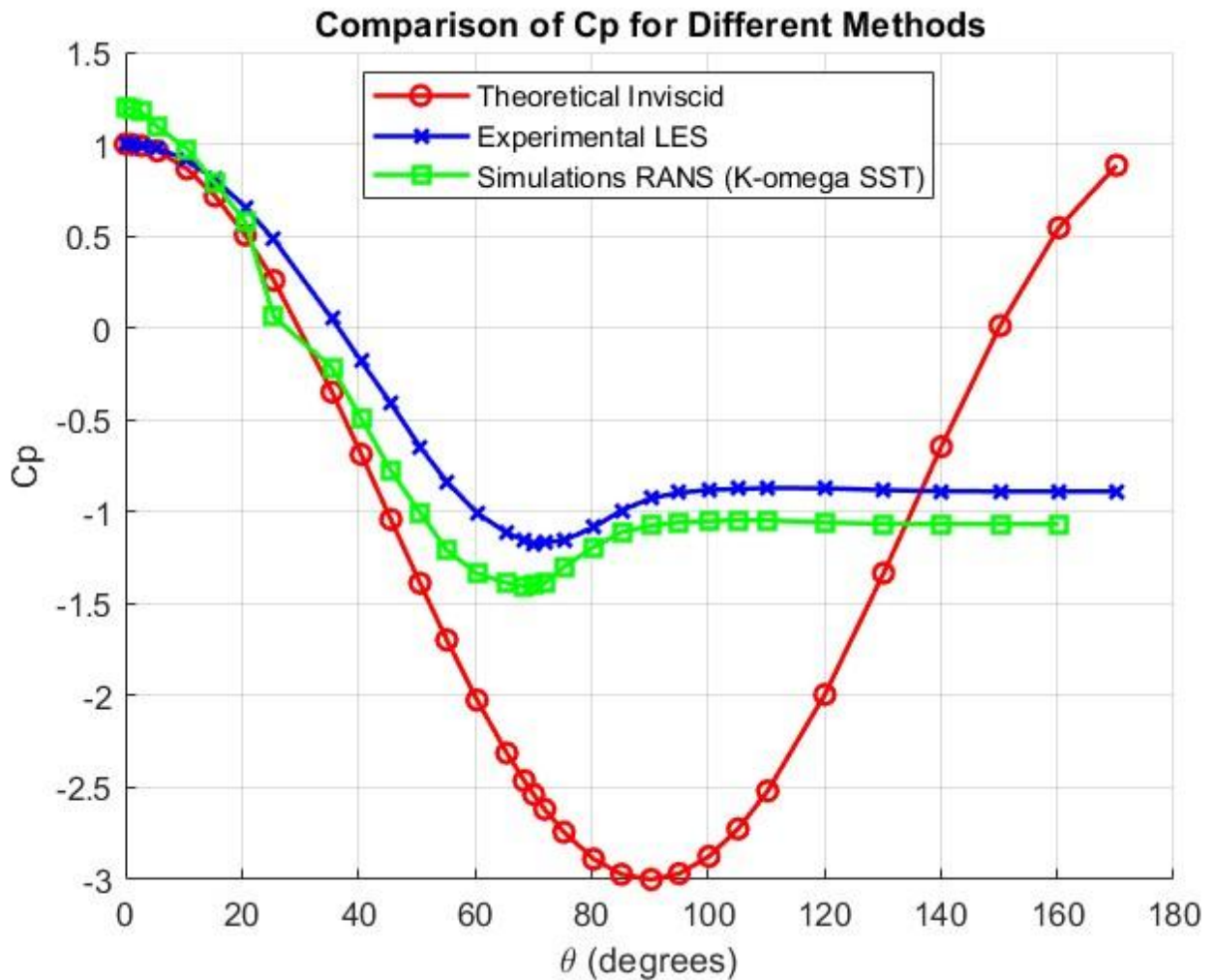


Figure 11 Comparison of C_p for different methods.

We can conclude that, the theoretical inviscid equation, provided a baseline understanding of the flow but lacked the flow capturing nature, which was captured in experimental and CFD study. The experimental data captured the data accurately and predicted the C_p representation around the cylinder on the most accurate way. While the k-omega SST model captured the general trend of the flow as it was dependent on the RANS equation, couldn't capture the flow as accurately as compared to the experimental data which was captured by an LES model.

6. REFERENCES

1. He, J., Zhao, W., Wan, D.: Numerical Calculations for Smooth Circular Cylinder Flow at 3900 Reynolds Numbers with SST-IDDES Turbulence Model.
2. Bayindir, C., Namli, B.: Efficient Sensing of the von Kármán Vortices Using Compressive Sensing. (2020)
3. Kravchenko, A.G., Moin, P.: Numerical studies of flow over a circular cylinder at $Re_D=3900$. *Physics of Fluids*. 12, 403–417 (2000). <https://doi.org/10.1063/1.870318>